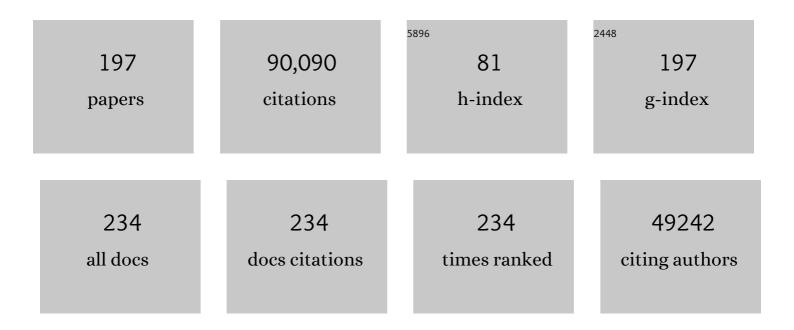
List of Publications by Year in descending order

Source: https://exaly.com/author-pdf/499075/publications.pdf Version: 2024-02-01



#	Article	lF	CITATIONS
1	Advances in functional and structural MR image analysis and implementation as FSL. NeuroImage, 2004, 23, S208-S219.	4.2	11,375
2	FSL. NeuroImage, 2012, 62, 782-790.	4.2	8,804
3	Improved Optimization for the Robust and Accurate Linear Registration and Motion Correction of Brain Images. NeuroImage, 2002, 17, 825-841.	4.2	8,296
4	Improved Optimization for the Robust and Accurate Linear Registration and Motion Correction of Brain Images. NeuroImage, 2002, 17, 825-841.	4.2	6,746
5	A global optimisation method for robust affine registration of brain images. Medical Image Analysis, 2001, 5, 143-156.	11.6	5,992
6	Tract-based spatial statistics: Voxelwise analysis of multi-subject diffusion data. NeuroImage, 2006, 31, 1487-1505.	4.2	5,755
7	The minimal preprocessing pipelines for the Human Connectome Project. Neurolmage, 2013, 80, 105-124.	4.2	4,042
8	A multi-modal parcellation of human cerebral cortex. Nature, 2016, 536, 171-178.	27.8	3,634
9	Bayesian analysis of neuroimaging data in FSL. NeuroImage, 2009, 45, S173-S186.	4.2	2,074
10	Evaluation of 14 nonlinear deformation algorithms applied to human brain MRI registration. NeuroImage, 2009, 46, 786-802.	4.2	1,988
11	A Bayesian model of shape and appearance for subcortical brain segmentation. NeuroImage, 2011, 56, 907-922.	4.2	1,937
12	Accurate, Robust, and Automated Longitudinal and Cross-Sectional Brain Change Analysis. NeuroImage, 2002, 17, 479-489.	4.2	1,828
13	Multilevel linear modelling for FMRI group analysis using Bayesian inference. NeuroImage, 2004, 21, 1732-1747.	4.2	1,476
14	Multimodal population brain imaging in the UK Biobank prospective epidemiological study. Nature Neuroscience, 2016, 19, 1523-1536.	14.8	1,414
15	General multilevel linear modeling for group analysis in FMRI. NeuroImage, 2003, 20, 1052-1063.	4.2	1,320
16	Image processing and Quality Control for the first 10,000 brain imaging datasets from UK Biobank. NeuroImage, 2018, 166, 400-424.	4.2	1,026
17	Advances in diffusion MRI acquisition and processing in the Human Connectome Project. NeuroImage, 2013, 80, 125-143.	4.2	851
18	The Human Connectome Project's neuroimaging approach. Nature Neuroscience, 2016, 19, 1175-1187.	14.8	825

#	Article	IF	CITATIONS
19	Functional connectomics from resting-state fMRI. Trends in Cognitive Sciences, 2013, 17, 666-682.	7.8	802
20	Common genetic variants influence human subcortical brain structures. Nature, 2015, 520, 224-229.	27.8	772
21	Anatomically related grey and white matter abnormalities in adolescent-onset schizophrenia. Brain, 2007, 130, 2375-2386.	7.6	718
22	Temporally-independent functional modes of spontaneous brain activity. Proceedings of the National Academy of Sciences of the United States of America, 2012, 109, 3131-3136.	7.1	696
23	The ENIGMA Consortium: large-scale collaborative analyses of neuroimaging and genetic data. Brain Imaging and Behavior, 2014, 8, 153-182.	2.1	696
24	Fast, automated,N-dimensional phase-unwrapping algorithm. Magnetic Resonance in Medicine, 2003, 49, 193-197.	3.0	637
25	Identification of common variants associated with human hippocampal and intracranial volumes. Nature Genetics, 2012, 44, 552-561.	21.4	594
26	MSM: A new flexible framework for Multimodal Surface Matching. NeuroImage, 2014, 100, 414-426.	4.2	532
27	Acquisition and voxelwise analysis of multi-subject diffusion data with Tract-Based Spatial Statistics. Nature Protocols, 2007, 2, 499-503.	12.0	526
28	Informatics and Data Mining Tools and Strategies for the Human Connectome Project. Frontiers in Neuroinformatics, 2011, 5, 4.	2.5	484
29	MIND: Modality independent neighbourhood descriptor for multi-modal deformable registration. Medical Image Analysis, 2012, 16, 1423-1435.	11.6	478
30	Normalized Accurate Measurement of Longitudinal Brain Change. Journal of Computer Assisted Tomography, 2001, 25, 466-475.	0.9	449
31	Social Network Size Affects Neural Circuits in Macaques. Science, 2011, 334, 697-700.	12.6	435
32	Medium-term effects of SARS-CoV-2 infection on multiple vital organs, exercise capacity, cognition, quality of life and mental health, post-hospital discharge. EClinicalMedicine, 2021, 31, 100683.	7.1	435
33	Evaluation of Registration Methods on Thoracic CT: The EMPIRE10 Challenge. IEEE Transactions on Medical Imaging, 2011, 30, 1901-1920.	8.9	363
34	Imaging dopamine receptors in humans with [11C]-(+)-PHNO: Dissection of D3 signal and anatomy. NeuroImage, 2011, 54, 264-277.	4.2	359
35	Human Connectome Project informatics: Quality control, database services, and data visualization. NeuroImage, 2013, 80, 202-219.	4.2	356
36	The developing human connectome project: A minimal processing pipeline for neonatal cortical surface reconstruction. NeuroImage, 2018, 173, 88-112.	4.2	315

#	Article	IF	CITATIONS
37	BIANCA (Brain Intensity AbNormality Classification Algorithm): A new tool for automated segmentation of white matter hyperintensities. NeuroImage, 2016, 141, 191-205.	4.2	308
38	Evaluating and reducing the impact of white matter lesions on brain volume measurements. Human Brain Mapping, 2012, 33, 2062-2071.	3.6	280
39	Connectivity-Based Functional Analysis of Dopamine Release in the Striatum Using Diffusion-Weighted MRI and Positron Emission Tomography. Cerebral Cortex, 2014, 24, 1165-1177.	2.9	276
40	The motor cortex shows adaptive functional changes to brain injury from multiple sclerosis. Annals of Neurology, 2000, 47, 606-613.	5.3	262
41	Novel genetic loci associated with hippocampal volume. Nature Communications, 2017, 8, 13624.	12.8	250
42	Diffusion imaging of whole, post-mortem human brains on a clinical MRI scanner. NeuroImage, 2011, 57, 167-181.	4.2	239
43	Multimodal surface matching with higher-order smoothness constraints. NeuroImage, 2018, 167, 453-465.	4.2	219
44	Fully Bayesian Spatio-Temporal Modeling of FMRI Data. IEEE Transactions on Medical Imaging, 2004, 23, 213-231.	8.9	218
45	BIDS apps: Improving ease of use, accessibility, and reproducibility of neuroimaging data analysis methods. PLoS Computational Biology, 2017, 13, e1005209.	3.2	218
46	Novel genetic loci underlying human intracranial volume identified through genome-wide association. Nature Neuroscience, 2016, 19, 1569-1582.	14.8	213
47	Physiological noise modelling for spinal functional magnetic resonance imaging studies. NeuroImage, 2008, 39, 680-692.	4.2	212
48	MRF-Based Deformable Registration and Ventilation Estimation of Lung CT. IEEE Transactions on Medical Imaging, 2013, 32, 1239-1248.	8.9	208
49	Classification and characterization of periventricular and deep white matter hyperintensities on MRI: A study in older adults. NeuroImage, 2018, 170, 174-181.	4.2	191
50	Distinction of seropositive NMO spectrum disorder and MS brain lesion distribution. Neurology, 2013, 80, 1330-1337.	1.1	189
51	Brain MRI atrophy quantification in MS. Neurology, 2017, 88, 403-413.	1.1	188
52	Structural MRI changes detectable up to ten years before clinical Alzheimer's disease. Neurobiology of Aging, 2012, 33, 825.e25-825.e36.	3.1	185
53	Physiological Noise in Brainstem fMRI. Frontiers in Human Neuroscience, 2013, 7, 623.	2.0	181
54	An evaluation of four automatic methods of segmenting the subcortical structures in the brain. NeuroImage, 2009, 47, 1435-1447.	4.2	180

#	Article	IF	CITATIONS
55	Combining shape and connectivity analysis: An MRI study of thalamic degeneration in Alzheimer's disease. NeuroImage, 2010, 49, 1-8.	4.2	171
56	Brainstem functional magnetic resonance imaging: Disentangling signal from physiological noise. Journal of Magnetic Resonance Imaging, 2008, 28, 1337-1344.	3.4	170
57	Manifestations of early brain recovery associated with abstinence from alcoholism. Brain, 2006, 130, 36-47.	7.6	169
58	Variability in fMRI: A reâ€examination of interâ€session differences. Human Brain Mapping, 2005, 24, 248-257.	3.6	162
59	fMRI reveals neural activity overlap between adult and infant pain. ELife, 2015, 4, .	6.0	161
60	Color of Scents: Chromatic Stimuli Modulate Odor Responses in the Human Brain. Journal of Neurophysiology, 2005, 93, 3434-3441.	1.8	155
61	Optimizing parameter choice for FSL-Brain Extraction Tool (BET) on 3D T1 images in multiple sclerosis. Neurolmage, 2012, 61, 1484-1494.	4.2	145
62	Fast, Fully Automated Global and Local Magnetic Field Optimization for fMRI of the Human Brain. NeuroImage, 2002, 17, 967-976.	4.2	143
63	Evaluating fibre orientation dispersion in white matter: Comparison of diffusion MRI, histology and polarized light imaging. NeuroImage, 2017, 157, 561-574.	4.2	141
64	In vivo identification of human cortical areas using high-resolution MRI: An approach to cerebral structure-function correlation. Proceedings of the National Academy of Sciences of the United States of America, 2003, 100, 2981-2986.	7.1	138
65	A combined post-mortem magnetic resonance imaging and quantitative histological study of multiple sclerosis pathology. Brain, 2012, 135, 2938-2951.	7.6	131
66	Hippocampal volume across age: Nomograms derived from over 19,700 people in UK Biobank. NeuroImage: Clinical, 2019, 23, 101904.	2.7	130
67	Targeting ASIC1 in primary progressive multiple sclerosis: evidence of neuroprotection with amiloride. Brain, 2013, 136, 106-115.	7.6	123
68	Multi-modal characterization of rapid anterior hippocampal volume increase associated with aerobic exercise. NeuroImage, 2016, 131, 162-170.	4.2	119
69	Brain surface contraction mapped in first-episode schizophrenia: a longitudinal magnetic resonance imaging study. Molecular Psychiatry, 2009, 14, 976-986.	7.9	117
70	Correspondences between retinotopic areas and myelin maps in human visual cortex. NeuroImage, 2014, 99, 509-524.	4.2	117
71	The effect of hypointense white matter lesions on automated gray matter segmentation in multiple sclerosis. Human Brain Mapping, 2012, 33, 2802-2814.	3.6	116
72	Association of Cardiovascular Risk Factors With MRI Indices of Cerebrovascular Structure and Function and White Matter Hyperintensities in Young Adults. JAMA - Journal of the American Medical Association, 2018, 320, 665.	7.4	105

#	Article	IF	CITATIONS
73	Towards Realtime Multimodal Fusion for Image-Guided Interventions Using Self-similarities. Lecture Notes in Computer Science, 2013, 16, 187-194.	1.3	104
74	Longitudinal and cross-sectional analysis of atrophy in Alzheimer's disease: Cross-validation of BSI, SIENA and SIENAX. NeuroImage, 2007, 36, 1200-1206.	4.2	100
75	Large-scale Probabilistic Functional Modes from resting state fMRI. NeuroImage, 2015, 109, 217-231.	4.2	98
76	Recommendations to improve imaging and analysis of brain lesion load and atrophy in longitudinal studies of multiple sclerosis. Journal of Neurology, 2013, 260, 2458-2471.	3.6	96
77	Structural changes of the brain in rheumatoid arthritis. Arthritis and Rheumatism, 2012, 64, 371-379.	6.7	95
78	White matter and lesion T1 relaxation times increase in parallel and correlate with disability in multiple sclerosis. Journal of Neurology, 2002, 249, 1279-1286.	3.6	94
79	Development of a functional magnetic resonance imaging simulator for modeling realistic rigid-body motion artifacts. Magnetic Resonance in Medicine, 2006, 56, 364-380.	3.0	91
80	Optimization of static field homogeneity in human brain using diamagnetic passive shims. Magnetic Resonance in Medicine, 2002, 48, 906-914.	3.0	89
81	Deep learning-based unlearning of dataset bias for MRI harmonisation and confound removal. NeuroImage, 2021, 228, 117689.	4.2	87
82	Independent anatomical and functional measures of the V1/V2 boundary in human visual cortex. Journal of Vision, 2005, 5, 1.	0.3	86
83	Comprehensive morphometry of subcortical grey matter structures in earlyâ€stage Parkinson's disease. Human Brain Mapping, 2014, 35, 1681-1690.	3.6	84
84	Assessment of physiological noise modelling methods for functional imaging of the spinal cord. NeuroImage, 2012, 60, 1538-1549.	4.2	83
85	Neuroanatomy of impaired self-awareness in Alzheimer's disease and mild cognitive impairment. Cortex, 2013, 49, 668-678.	2.4	83
86	Construction of a neonatal cortical surface atlas using Multimodal Surface Matching in the Developing Human Connectome Project. NeuroImage, 2018, 179, 11-29.	4.2	83
87	Study protocol: the Whitehall II imaging sub-study. BMC Psychiatry, 2014, 14, 159.	2.6	82
88	Challenges in the reproducibility of clinical studies with resting state fMRI: An example in early Parkinson's disease. NeuroImage, 2016, 124, 704-713.	4.2	81
89	The developing Human Connectome Project (dHCP) automated resting-state functional processing framework for newborn infants. NeuroImage, 2020, 223, 117303.	4.2	81
90	Lesion probability mapping to explain clinical deficits and cognitive performance in multiple sclerosis. Multiple Sclerosis Journal, 2011, 17, 681-689.	3.0	79

#	Article	IF	CITATIONS
91	Learning patterns of the ageing brain in MRI using deep convolutional networks. NeuroImage, 2021, 224, 117401.	4.2	79
92	Gray matter volume is associated with rate of subsequent skill learning after a long term training intervention. Neurolmage, 2014, 96, 158-166.	4.2	78
93	Quantitative assessment of the susceptibility artefact and its interaction with motion in diffusion MRI. PLoS ONE, 2017, 12, e0185647.	2.5	72
94	Common Genetic Variation Indicates Separate Causes for Periventricular and Deep White Matter Hyperintensities. Stroke, 2020, 51, 2111-2121.	2.0	71
95	Cross-species cortical alignment identifies different types of anatomical reorganization in the primate temporal lobe. ELife, 2020, 9, .	6.0	71
96	Applying FSL to the FIAC data: Model-based and model-free analysis of voice and sentence repetition priming. Human Brain Mapping, 2006, 27, 380-391.	3.6	69
97	Automatic segmentation of the striatum and globus pallidus using MIST: Multimodal Image Segmentation Tool. NeuroImage, 2016, 125, 479-497.	4.2	66
98	Conditioned respiratory threat in the subdivisions of the human periaqueductal gray. ELife, 2016, 5, .	6.0	66
99	Functional subdivision of the human periaqueductal grey in respiratory control using 7tesla fMRI. NeuroImage, 2015, 113, 356-364.	4.2	64
100	Perturbation method for magnetic field calculations of nonconductive objects. Magnetic Resonance in Medicine, 2004, 52, 471-477.	3.0	61
101	Meaningful design and contrast estimability in FMRI. NeuroImage, 2007, 34, 127-136.	4.2	60
102	Resting Functional Connectivity Reveals Residual Functional Activity in Alzheimer's Disease. Biological Psychiatry, 2013, 74, 375-383.	1.3	59
103	Automated segmentation of the substantia nigra, subthalamic nucleus and red nucleus in 7 T data at young and old age. NeuroImage, 2016, 139, 324-336.	4.2	57
104	Two-dimensional population map of cortical connections in the human internal capsule. Journal of Magnetic Resonance Imaging, 2007, 25, 48-54.	3.4	56
105	A consistent relationship between local white matter architecture and functional specialisation in medial frontal cortex. NeuroImage, 2006, 30, 220-227.	4.2	53
106	Sharing brain mapping statistical results with the neuroimaging data model. Scientific Data, 2016, 3, 160102.	5.3	53
107	Whole-brain magnetic resonance spectroscopic imaging measures are related to disability in ALS. Neurology, 2013, 80, 610-615.	1.1	50
108	Reducing distortions in diffusionâ€weighted echo planar imaging with a dualâ€echo blipâ€reversed sequence. Magnetic Resonance in Medicine, 2010, 64, 382-390.	3.0	49

#	Article	IF	CITATIONS
109	Denoising spinal cord fMRI data: Approaches to acquisition and analysis. NeuroImage, 2017, 154, 255-266.	4.2	49
110	Stimulus Site and Modality Dependence of Functional Activity within the Human Spinal Cord. Journal of Neuroscience, 2012, 32, 6231-6239.	3.6	47
111	Dissecting the pathobiology of altered MRI signal in amyotrophic lateral sclerosis: A post mortem whole brain sampling strategy for the integration of ultra-high-field MRI and quantitative neuropathology. BMC Neuroscience, 2018, 19, 11.	1.9	47
112	Imaging Surrogates of Disease Activity in Neuromyelitis Optica Allow Distinction from Multiple Sclerosis. PLoS ONE, 2015, 10, e0137715.	2.5	47
113	Magnetic resonance imaging in late-life depression: vascular and glucocorticoid cascade hypotheses. British Journal of Psychiatry, 2012, 201, 46-51.	2.8	44
114	The Developing Human Connectome Project Neonatal Data Release. Frontiers in Neuroscience, 2022, 16,	2.8	42
115	Artificial intelligence for clinical decision support in neurology. Brain Communications, 2020, 2, fcaa096.	3.3	41
116	Comparison and Evaluation of Segmentation Techniques for Subcortical Structures in Brain MRI. Lecture Notes in Computer Science, 2008, 11, 409-416.	1.3	40
117	White Matter Imaging Correlates of Early Cognitive Impairment Detected by the Montreal Cognitive Assessment After Transient Ischemic Attack and Minor Stroke. Stroke, 2017, 48, 1539-1547.	2.0	38
118	Quantifying the pattern of optic tract degeneration in human hemianopia. Journal of Neurology, Neurosurgery and Psychiatry, 2014, 85, 379-386.	1.9	33
119	Optimizing full-brain coverage in human brain MRI through population distributions of brain size. NeuroImage, 2014, 98, 513-520.	4.2	33
120	Simulating the effects of time-varying magnetic fields with a realistic simulated scanner. Magnetic Resonance Imaging, 2010, 28, 1014-1021.	1.8	32
121	Automated lesion segmentation with BIANCA: Impact of population-level features, classification algorithm and locally adaptive thresholding. NeuroImage, 2019, 202, 116056.	4.2	32
122	Multimodal Surface Matching: Fast and Generalisable Cortical Registration Using Discrete Optimisation. Lecture Notes in Computer Science, 2013, 23, 475-486.	1.3	32
123	Allostatic load as a predictor of grey matter volume and white matter integrity in old age: The Whitehall II MRI study. Scientific Reports, 2018, 8, 6411.	3.3	31
124	Quantitative FLAIR MRI in Amyotrophic Lateral Sclerosis. Academic Radiology, 2017, 24, 1187-1194.	2.5	31
125	Alteration to hippocampal volume and shape confined to cannabis dependence: a multiâ€site study. Addiction Biology, 2019, 24, 822-834.	2.6	30
126	Triplanar ensemble U-Net model for white matter hyperintensities segmentation on MR images. Medical Image Analysis, 2021, 73, 102184.	11.6	29

#	Article	IF	CITATIONS
127	Motion Correction and Parameter Estimation in dceMRI Sequences: Application to Colorectal Cancer. Lecture Notes in Computer Science, 2011, 14, 476-483.	1.3	28
128	Globally Optimal Deformable Registration on a Minimum Spanning Tree Using Dense Displacement Sampling. Lecture Notes in Computer Science, 2012, 15, 115-122.	1.3	28
129	Target Identification for Stereotactic Thalamotomy Using Diffusion Tractography. PLoS ONE, 2012, 7, e29969.	2.5	28
130	Protocol to determine the optimal intraoral passive shim for minimisation of susceptibility artifact in human inferior frontal cortex. NeuroImage, 2003, 19, 1802-1811.	4.2	26
131	Generalised Overlap Measures for Assessment of Pairwise and Groupwise Image Registration and Segmentation. Lecture Notes in Computer Science, 2005, 8, 99-106.	1.3	26
132	Quantitative Susceptibility Mapping by Inversion of a Perturbation Field Model: Correlation With Brain Iron in Normal Aging. IEEE Transactions on Medical Imaging, 2015, 34, 339-353.	8.9	26
133	A Framework for Detailed Objective Comparison of Non-rigid Registration Algorithms in Neuroimaging. Lecture Notes in Computer Science, 2004, , 679-686.	1.3	25
134	Contrasting the brain imaging features of MOG-antibody disease, with AQP4-antibody NMOSD and multiple sclerosis. Multiple Sclerosis Journal, 2022, 28, 217-227.	3.0	24
135	Integrating temporal information with a non-rigid method of motion correction for functional magnetic resonance images. Image and Vision Computing, 2007, 25, 311-320.	4.5	23
136	Novel Fast Marching for Automated Segmentation of the Hippocampus (FMASH): Method and validation on clinical data. NeuroImage, 2011, 55, 1009-1019.	4.2	23
137	Optimising neonatal fMRI data analysis: Design and validation of an extended dHCP preprocessing pipeline to characterise noxious-evoked brain activity in infants. NeuroImage, 2019, 186, 286-300.	4.2	22
138	Detection of Alzheimer's Disease using cortical diffusion tensor imaging. Human Brain Mapping, 2021, 42, 967-977.	3.6	22
139	Non-local Shape Descriptor: A New Similarity Metric for Deformable Multi-modal Registration. Lecture Notes in Computer Science, 2011, 14, 541-548.	1.3	22
140	Relating diffusion tensor imaging measurements to microstructural quantities in the cerebral cortex in multiple sclerosis. Human Brain Mapping, 2019, 40, 4417-4431.	3.6	21
141	Can correcting feature location in simulated mean climate improve agreement on projected changes?. Geophysical Research Letters, 2013, 40, 354-358.	4.0	20
142	SIENAâ€XL for improving the assessment of gray and white matter volume changes on brain MRI. Human Brain Mapping, 2018, 39, 1063-1077.	3.6	20
143	Optimal echo time for functional MRI of the infant brain identified in response to noxious stimulation. Magnetic Resonance in Medicine, 2017, 78, 625-631.	3.0	19
144	Separation of trait and state in stuttering. Human Brain Mapping, 2018, 39, 3109-3126.	3.6	19

MARK JENKINSON

#	Article	IF	CITATIONS
145	HIV Distal Neuropathic Pain Is Associated with Smaller Ventral Posterior Cingulate Cortex. Pain Medicine, 2017, 18, pnw180.	1.9	17
146	Optimizing image registration and infarct definition in stroke research. Annals of Clinical and Translational Neurology, 2017, 4, 166-174.	3.7	17
147	Donepezil Enhances Frontal Functional Connectivity in Alzheimer's Disease: A Pilot Study. Dementia and Geriatric Cognitive Disorders Extra, 2017, 6, 518-528.	1.3	17
148	Fronto-parietal involvement in chronic stroke motor performance when corticospinal tract integrity is compromised. NeuroImage: Clinical, 2021, 29, 102558.	2.7	17
149	Structural and functional bases of visuospatial associative memory in older adults. Neurobiology of Aging, 2013, 34, 961-972.	3.1	15
150	Optimizing RetrolCor and RetroKCor corrections for multi-shot 3D FMRI acquisitions. Neurolmage, 2014, 84, 394-405.	4.2	15
151	Quantitative Susceptibility Mapping for Characterization of Intraplaque Hemorrhage and Calcification in Carotid Atherosclerotic Disease. Journal of Magnetic Resonance Imaging, 2020, 52, 534-541.	3.4	15
152	A Marginalized MAP Approach and EM Optimization for Pair-Wise Registration. Lecture Notes in Computer Science, 2007, 20, 662-674.	1.3	15
153	Subcortical segmentation of the fetal brain in 3D ultrasound using deep learning. NeuroImage, 2022, 254, 119117.	4.2	15
154	Quantifying Infarct Growth and Secondary Injury Volumes. Stroke, 2018, 49, 1647-1655.	2.0	14
155	Spatial Warping Network for 3D Segmentation of the Hippocampus in MR Images. Lecture Notes in Computer Science, 2019, , 284-291.	1.3	14
156	White matter hyperintensities classified according to intensity and spatial location reveal specific associations with cognitive performance. NeuroImage: Clinical, 2021, 30, 102616.	2.7	13
157	Brain Tumour Segmentation Using aÂTriplanar Ensemble of U-Nets on MR Images. Lecture Notes in Computer Science, 2021, , 340-353.	1.3	12
158	Feasibility of Diffusion Tensor and Morphologic Imaging of Peripheral Nerves at Ultra-High Field Strength. Investigative Radiology, 2018, 53, 705-713.	6.2	11
159	Edge- and Detail-Preserving Sparse Image Representations for Deformable Registration of Chest MRI and CT Volumes. Lecture Notes in Computer Science, 2013, 23, 463-474.	1.3	11
160	Cortical diffusivity investigation in posterior cortical atrophy and typical Alzheimer's disease. Journal of Neurology, 2021, 268, 227-239.	3.6	10
161	Integrating large-scale neuroimaging research datasets: Harmonisation of white matter hyperintensity measurements across Whitehall and UK Biobank datasets. NeuroImage, 2021, 237, 118189.	4.2	10
162	Opportunities for Understanding MS Mechanisms and Progression With MRI Using Large-Scale Data Sharing and Artificial Intelligence. Neurology, 2021, 97, 989-999.	1.1	10

MARK JENKINSON

#	Article	IF	CITATIONS
163	The impact of transfer learning on <scp>3D</scp> deep learning convolutional neural network segmentation of the hippocampus in mild cognitive impairment and Alzheimer disease subjects. Human Brain Mapping, 2022, 43, 3427-3438.	3.6	10
164	Modelling the distribution of white matter hyperintensities due to ageing on MRI images using Bayesian inference. NeuroImage, 2019, 185, 434-445.	4.2	9
165	Machine Learning Quantitation of Cardiovascular and Cerebrovascular Disease: A Systematic Review of Clinical Applications. Diagnostics, 2021, 11, 551.	2.6	9
166	Comparison of domain adaptation techniques for white matter hyperintensity segmentation in brain MR images. Medical Image Analysis, 2021, 74, 102215.	11.6	9
167	One-year changes in brain microstructure differentiate preclinical Huntington's disease stages. NeuroImage: Clinical, 2020, 25, 102099.	2.7	8
168	Unlearning Scanner Bias for MRI Harmonisation. Lecture Notes in Computer Science, 2020, , 369-378.	1.3	8
169	Intracortical diffusion tensor imaging signature of microstructural changes in frontotemporal lobar degeneration. Alzheimer's Research and Therapy, 2021, 13, 180.	6.2	8
170	Atlas-Based Improved Prediction of Magnetic Field Inhomogeneity for Distortion Correction of EPI Data. Lecture Notes in Computer Science, 2009, 12, 951-959.	1.3	7
171	Performance of single spin-echo and doubly refocused diffusion-weighted sequences in the presence of eddy current fields with multiple components. Magnetic Resonance Imaging, 2011, 29, 659-667.	1.8	7
172	Evidence for a novel subcortical mechanism for posterior cingulate cortex atrophy in HIV peripheral neuropathy. Journal of NeuroVirology, 2020, 26, 530-543.	2.1	7
173	TIGER – A New Model for Spatio-temporal Realignment of FMRI Data. Lecture Notes in Computer Science, 2004, , 292-303.	1.3	7
174	Methods for Tractography-Driven Surface Registration of Brain Structures. Lecture Notes in Computer Science, 2009, 12, 705-712.	1.3	6
175	A saliency-based hierarchy for local symmetries. Image and Vision Computing, 2002, 20, 85-101.	4.5	5
176	Fieldmap-Free Retrospective Registration and Distortion Correction for EPI-Based Functional Imaging. Lecture Notes in Computer Science, 2008, 11, 271-279.	1.3	5
177	Textural mutual information based on cluster trees for multimodal deformable registration. , 2012, , .		5
178	Construction of a neonatal cortical surface atlas using multimodal surface matching. , 2016, , .		5
179	Can correcting feature location in simulated mean climate improve agreement on projected changes?. Geophysical Research Letters, 2013, 40, 354.	4.0	5
180	Correcting precipitation feature location in general circulation models. Journal of Geophysical Research D: Atmospheres, 2014, 119, 13,350.	3.3	4

#	Article	IF	CITATIONS
181	SIENA: Single and multiple time point brain atrophy analysis. NeuroImage, 2001, 13, 250.	4.2	3
182	Assessing Reliability of Myocardial Blood Flow After Motion Correction With Dynamic PET Using a Bayesian Framework. IEEE Transactions on Medical Imaging, 2019, 38, 1216-1226.	8.9	3
183	Elucidating distinct clinico-radiologic signatures in the borderland between neuromyelitis optica and multiple sclerosis. Journal of Neurology, 2022, 269, 269-279.	3.6	3
184	Reducing Activation-Related Bias in FMRI Registration. Lecture Notes in Computer Science, 2004, , 278-285.	1.3	3
185	Exploratory motion analysis in fMRI using ICA. NeuroImage, 2001, 13, 69.	4.2	2
186	MR-DTI and PET multimodal imaging of dopamine release within subdivisions of basal ganglia. Journal of Physics: Conference Series, 2011, 317, 012005.	0.4	2
187	Unlearning Scanner Bias for MRI Harmonisation in Medical Image Segmentation. Communications in Computer and Information Science, 2020, , 15-25.	0.5	2
188	The Impact of Heterogeneity and Uncertainty on Prediction of Response to Therapy Using Dynamic MRI Data. Lecture Notes in Computer Science, 2013, 16, 316-323.	1.3	2
189	MRI Brain T1 Relaxation Time Changes in MS Patients Increase Over Time in Both the White Matter and the Cortex. , 2003, 13, 234-239.		2
190	Iterative Dual LDA: A Novel Classification Algorithm for Resting State fMRI. Lecture Notes in Computer Science, 2016, , 279-286.	1.3	2
191	Increasing the detectability of external influence on precipitation by correcting feature location in GCMs. Journal of Geophysical Research D: Atmospheres, 2014, 119, 12,466.	3.3	1
192	Omni-Supervised Domain Adversarial Training for White Matter Hyperintensity Segmentation in the UK Biobank. , 2022, , .		1
193	High Resolution Boundary Element Forward Models for Sensor Arrays: An Application to Electroencephalography. , 0, , .		0
194	Non-Rigid Motion Estimation and Spatio-Temporal Realignment in FMRI. , 0, , .		0
195	A combined diffusion tensor imaging (DTI) and [11C]-(+)-PHNO positron emission tomography (PET) study to quantify dopamine D3/D2 receptors in pallidum. NeuroImage, 2010, 52, S23.	4.2	0
196	FAST-IT: <i>F</i> ind <i>A S</i> imple <i>T</i> est â€" <i>I</i> n <i>T</i> IA (transient ischaemic attack): a prospective cohort study to develop a multivariable prediction model for diagnosis of TIA through proteomic discovery and candidate lipid mass spectrometry, neuroimaging and machine learningâ€"study protocol. BMJ Open, 2022, 12, e045908.	1.9	0
197	Optimization of the MR imaging pipeline using simulation. , 2022, , 165-193.		0